J Radioanal Nucl Chem (2013) 296:1079–1084
DOI 10.1007/s10967-012-2135-x

Radio-microanalytical particle measurements method and application to Fukushima aerosols collected in Japan

C. J. Zeissler · L. P. G. Forsley · R. M. Lindstrom · S. Newsome · A. Kirk · P. A. Mosier-Boss

Received: 31 July 2012 / Published online: 26 August 2012

Abstract A nondestructive analytical method based on autoradiography and gamma spectrometry was developed to perform activity distribution analysis for particulate samples. This was applied to aerosols collected in Fukushima Japan, 40 km north of the Daiichi nuclear power plant for a 6 week period beginning shortly after the March 2011 tsunami. For an activity distribution of 990 "hot particles" from a small filter area, the hottest particle was nearly one Bq $^{137+134}$Cs but most of the activity in the filter was produced by particles having <50 mBq each. ^{134}Cs/^{137}Cs activity ratios corrected to March 20, 2011 ranged from 0.68 (u_c = 28 %) to 1.3 (u_c = 15 %). The average ratio for a large quantity of particles was 0.92 (u_c = 4 %). Virtually all activity collected was beta and not alpha, suggesting little if any direct fuel debris was present at this site and time. These findings are expected to assist with separate efforts to better understand the emission events, radionuclide transport and potential environmental or biological uptake. The methods should be applicable to general environmental, radiotoxicological and similar studies for which activity distribution and particle chemistry are of importance.

Keywords Activity · Radiocesium · Detection limit · Fukushima · Imaging plate autoradiography · Particle size distribution

Introduction

A tsunami struck the Daiichi nuclear power plant in Japan on Friday March 11, 2011, shortly followed by a series of radioisotope release events [1]. Radiological emissions could conceivably be original fuel material, their fission products or activation products, all of which have been detected at one time or another in various samples attributed to the plant. The ^{134}Cs/^{137}Cs ratio was slightly below 1 shortly after the tsunami [2] indicating fresh release.

Particle sizes and chemistry are relevant to transport, chemical, environmental and biological uptake mechanisms, ultimately impacting the fate, toxicity and remediation issues of emitted radionuclides. The combined analytical methods of autoradiography, gamma spectrometry and microscopy provide a means to assess these characteristics.

Experimental methods

After the tsunami event, aerosols were incidentally collected for a duration of about 6 weeks between April 2011 and May 2011 by air filters in a control module used to operate a small tethered robotic submarine known as a

C. J. Zeissler (✉) · R. M. Lindstrom
National Institute of Standards & Technology (NIST),
100 Bureau Dr., Gaithersburg, MD 20899, USA
e-mail: cynthia.zeissler@nist.gov

L. P. G. Forsley · A. Kirk
JWK International Corporation, Annandale, VA 22003, USA

S. Newsome
SeaBotix Inc., 2877 Historic Decatur Rd. Suite 100,
San Diego, CA 92106, USA

P. A. Mosier-Boss
Research Laboratory of Electronics, Massachusetts Institute of Technology, Cambridge, MA 02139, USA

"little benthic vessel" (LBV, SeaBotix Inc.[1]) [3]. The LBV work was performed to scan for obstructions that might hamper ship movements in a harbor near Soma, Fukushima Prefecture, Japan, 40 km north of the Daiichi nuclear power plant. In comparison, the closest radionuclide international monitoring system station (IMS) to the Daiichi plant was 250 km to the southwest of the Daiichi plant (station RN38 or JPP38) [2]. Since the LBV console aerosol collection was unplanned prior to the crisis, the air volume and collection efficiencies of the equipment are not known precisely. Using fan specifications and filter characteristics, it is estimated approximately 10^5 m^3 of air were sampled assuming a 100 % duty cycle and that the filter collection efficiency was at least 85 %.

The LBV was scanned for radiation in Japan by the shipper, then shipped to the USA where the interior was scanned for radiation using an alpha/beta/gamma frisker. Inlet and outlet filters from the electronics console of the LBV were gamma counted and then divided into quarters. A portion was briefly counted by alpha–beta liquid scintillation. A one-quarter portion of each filter was sent to NIST for radio-microanalysis.

Liquid scintillation counting and gamma spectrometry

Whole filter samples or subportions were analyzed with a shielded Ortec 18 % HPGe cryo-cooled Be-window gamma spectrometer, a Compton-suppressed HPGe detector, and/or a Beckman LS6500 alpha beta liquid scintillator. Sample subportions were quantitatively measured at NIST for 1–4 days with a low-background Ge detector (relative efficiency 117 %, resolution 1.9 keV fwhm at 1.33 MeV) shielded by 15 cm of pre-WWII iron. The net areas and uncertainties for peaks at 662 (for ^{137}Cs) and 796 keV (for ^{134}Cs) were obtained with a fixed-boundary integration routine [4]. Counting rates were converted to disintegration rates via an efficiency-energy calibration using NIST Standard Reference Material (SRM) 4218 ^{152}Eu at 10 cm, and adjusting to 0 cm using the measured axial gradient for ^{137}Cs. Corrections were made for cascade summing. Uncertainties for gamma data include counting statistics (Type A) and geometrical considerations (Type B), added in quadrature and reported as relative uncertainties at the combined standard uncertainty level ($k = 1$). The date of March 20, 2011, close to the onset of collection, is used for many of the reported activity values.

[1] Certain commercial equipment, instruments or materials are identified to specify experimental procedures. Such identification does not imply recommendation or endorsement by the National Institute of Standards and Technology, nor does it imply that the materials or equipment identified are necessarily the best available for the purpose.

Autoradiography

Autoradiography using phosphor imaging plates provides a means to assess activity levels with spatial distribution information [5, 6]. This was applied to the air filter samples using nominally 2 μm thick Mylar films for contamination control. Dispersions to improve geometrical detection efficiency and spatial resolution were made by a dry technique to avoid radionuclide mobilization or other changes using optically clear adhesive tape [7, 8]. A sequential stripping approach was used to gradually disperse the filter fibers and particulate matter over increasingly more tape area. Material affixed between tape and protective static-dissipative Mylar films in the form of counting frames [8] were pressed against the imaging plate with a foam pad within an exposure cassette. Plate handling and exposures were performed in the dark at 19.0 °C. This configuration produces a geometrical collection efficiency of 50 %, approaching 100 % when samples are sandwiched between two facing plates.

The imaging plate autoradiography system used was a BAS-5000 (Fuji Medical Systems, Tokyo, Japan). Laser scanner settings were sensitivity $S = 30{,}000$ and pixel size = 25 μm. These settings using "TR" phosphor plates are capable of detecting individual alpha-particles and beta-particles [9]. Micromanipulation with needles and similar tools on a microscope with iterative autoradiography was used to isolate individual particles for microscopy and to verify activity was not lost in the process.

Calculation of activity from phosphor luminescence

Suitable point source standards for high resolution quantitative autoradiography were unavailable, so gamma spectrometry was used to determine the activity level of particles measured by autoradiography by making a calibration curve to relate autoradiography results to activity. Autoradiography image intensity was measured in units of standardized photostimulable luminescence of the phosphor (PSL) which is linear as a function of dose [10], by instrument-dedicated software ImageGauge version 3.46 (Fuji Photo Film Co., Ltd.). Individually localized radioisotope emissions ("counts") were classified on the basis of their PSL value as either alpha or beta using a pixel summing spectral technique [9], verified by absorption testing and independent gamma spectrometry.

Spatial clusters of counts recorded in an autoradiograph identify the presence of hot particles. To measure the intensity of an individual hot particle, an imaging plate background value B in PSL/mm^2 was obtained by selecting a relatively large area of the autoradiograph (typically about 5,000 mm^2) in a control region away from the sample exposed to the same amount of background. The PSL values

for the pixels in a circular area enclosing the cluster representing the hot particle were summed to produce PSL_c for a circular area A_c (mm^2). Background was subtracted from the measurement according to Eq. 1 to produce the PSL value for the particle, PSL_p as measured at that A_c.

$$PSL_p = PSL_c - (A_c * B). \quad (1)$$

Of significance was the development of a method for correcting PSL_p data to make comparable measurements of multiple hot particles in spatially crowded fields. The radius of the area A_c is the radial distance r from the center of the corresponding hot particle. The relationship between PSL_p and r was found by making many measurements of different A_c for the same particle and fitting the resulting table of A_c versus PSL_p data using MatLab version 7.8.0.347 (R2009a) (The MathWorks, Inc., Natick, MA, USA). When hot particles were crowded together, a large A_c could not be used without sometimes accidentally incorporating some activity from nearby hot particles. As given in a later example, by using a small A_c instead, the measurement can avoid nearby hot particles. However, many of the peripheral counts in the autoradiograph that belong to the hot particle will often not be included in small A_c areas. To correct for this, an A_c versus PSL_p relationship was found that provided a means to measure pixel intensity in a small area centered on the hot spot, after which a correction can be applied to determine the PSL_p as if all of the counts had been included in the measurement. That is, by measuring PSL_p for a small A_c one can calculate the PSL_p for a larger A_c and thus the total intensity I for the hot particle.

Once the I of a hot particle had been determined it was converted into true activity in units of Bq using an I-to-Bq calibration curve. This calibration curve was produced by counting the same specimens by autoradiography and gamma spectrometry independently, taking care to adjust the Bq values determined by gamma spectrometry to the same date of the autoradiography measurement.

In all measurements for which I conversion to activity in Bq was used, or for measurements where the I of one hot particle was compared to the I of another hot particle (as was done in creating activity distribution curves), the phenomenon known as phosphor fading [11] was normalized out by performing all measurements with the same sample exposure time.

Conversion of activity to minimum particle diameter

The specific activity of the radionuclide in Bq/g can be used to calculate an equivalent spherical diameter for each radioactive point source using the measured activity, specific gravity of the material comprising the particle in g/cm^3 and weight fraction of the radionuclide in the particle. The following equations can be used to relate the activity from a point source to an equivalent spherical diameter:

$$V = \frac{X}{\mathrm{SA} * W * \rho} \quad (2)$$

$$\mathrm{SA} = \frac{(\ln 2) * A_V}{t_{1/2} * M} \quad (3)$$

$$V = \frac{4}{3} * \pi * (d/2)^3 \quad (4)$$

$$d = 2 * \sqrt[3]{\frac{3 * X}{4 * \pi * \mathrm{SA} * W * \rho}} \quad (5)$$

where V is the spherical particle volume, X is the activity of the particle, W is the weight fraction of the radioactive element in the particle, ρ is the density of the particle in g/cm^3, SA is the specific activity of the radionuclide, A_v is Avogadro's number $= 6.022 \times 10^{23}$, $t_{1/2}$ is the half-life of the radionuclide, M is the atomic mass of the radionuclide and d is the diameter of the spherical particle. Equations 2 and 4 were set equal to each other and then solved for the diameter to obtain Eq. 5.

In order to calculate d when the exact chemical compound is not known, the reasonable range of possibilities may be considered. The most important limiting case would be a dense compound with a high wt% of the radionuclide. At the other extreme, the radionuclide might occur as a condensate on the surface of a chemically unrelated material or be incidentally entrained at low concentration inside of another material having low density. For this reason, calculated diameters are always a minimum size until verified by microscopy or other means.

For cesium activity examined in this work, the contribution of ^{134}Cs ($t_{1/2} = 2.1$ years) is negligible to the mass of a particle relative to ^{137}Cs ($t_{1/2} = 30$ years) due to the difference in half-lives. The densities of likely cesium salts such as cesium hydroxide (CsOH) or cesium oxide (Cs_2O) through cesium uranate (Cs_2UO_4) range from a low of 3.68 to 6.65 g/cm^3. These same materials have cesium mass fractions ranging from 0.94 to 0.47 g/g. Calculated diameters of equivalent spheres for this range of values do not vary much, and are about 0.5 ± 0.05 μm for 0.5 Bq of ^{137}Cs, with the smallest calculated equivalent sphere being 0.45 μm for the Cs_2O case not taking into account hydration.

Results

Both, the radiation scanning performed on the LBV by the shipper in Japan, and frisking of the LBV after reception in the US, detected nothing above background. The inlet filter removed from the LBV's electronics control console was gamma counted whole prior to delivery to NIST for

5.53×10^4 s in late June 2011, which identified ^{134}Cs, ^{137}Cs and ^{40}K. The ^{134}Cs was detected as nine gamma lines of which there were 1.15×10^5 counts at 605 keV and 7.71×10^4 counts at 796 keV. ^{137}Cs was detected as 1.08×10^5 counts at 661 keV. ^{40}K which is common in natural environmental samples was 4.11×10^1 counts at 1,460 keV. No counts above background were detected in a control filter after a 7.17×10^4 s count.

After dividing the filter into four equal parts, 10 min of liquid alpha/beta scintillation counting was performed on one of the quarters of the original whole filter. No net measurable alpha activity was detected.

A 17 h autoradiograph of another one of the quarters of the original whole inlet filter was performed. This detected many discrete points of activity, correlating with visible soiling present on the filter (Fig. 1), whereas no activity was detected in the control filter. The radiation counts that comprised the discrete points of activity each had an intensity ranging from about 0.01 to 0.11 PSL, consistent with a beta signature [9]. Discrete counts 0.2 PSL or higher, indicative of alpha, were not found above background. Images could also be reproduced through 25 μm aluminum foil, validating the beta dominance.

Portion "e" of the inlet filter, 2.7 cm^2 representing roughly 10^4 m^3 air (Fig. 1), was separated from the remaining filter material and dispersed onto 25 pieces of sticky tape and exposed to an imaging plate (Fig. 2). Several exposures using counting times ranging from 20 min to 57 days demonstrated that the number of particles found was dependent on exposure time. The longer the exposure, the more particles were detected, suggesting the population was rich in low-activity particles. This finding was verified once the activity distribution was measured later.

Several of the hottest particles found in sector "e" were physically isolated from other dispersed material by successive micromanipulation and autoradiography. Isolated particles were measured independently by gamma spectrometry. A 1 h autoradiograph of the hottest particle (0.9 Bq) is shown in the Fig. 3 inset.

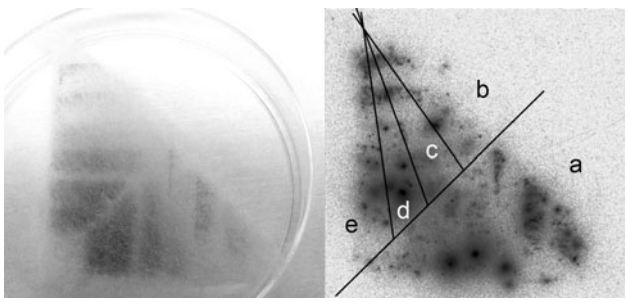

Fig. 1 A quarter section of the inlet filter (*left*) and its 17 h autoradiograph (*right*). The filter quarter is 6.5 × 6.5 × 9.4 cm. The *black* lines indicate where the filter was divided to perform dispersions. Portion "*e*" was dispersed onto 25 pieces of tape

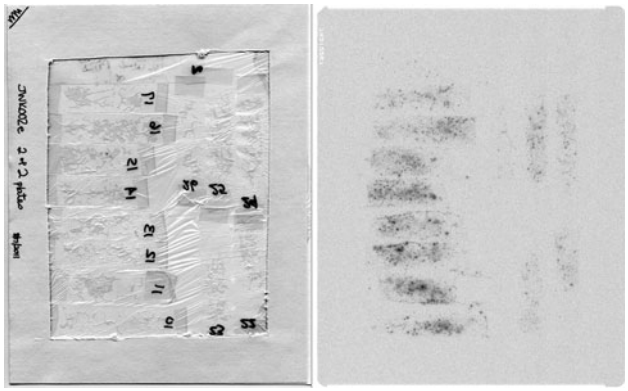

Fig. 2 17 h exposure autoradiograph of half of the dispersal tapes from section "e" of the inlet filter. *Left*, a counting frame of tapes and *right* autoradiograph. Both images are 20 cm wide

The phosphor plate intensity versus measurement area tests produced PSL_p/A_c curves such as the one shown in Fig. 3, where the area shown as "a" in the inset is $A_c = 1.26$ mm^2. Area "a" fails to include all of the beta counts (dark spots) and corresponds to the high-slope portion (left side) of the PSL_p/A_c plot. In comparison, the encircled area "b" of $A_c = 22.82$ mm^2 on the other side of the inflection point of the curve appears to enclose most of the beta counts. Tests with other particles and exposure times found the overall shape of the PSL_p versus A_c relationship to be independent of exposure time, activity level and radionuclide type and was described by Eq. 6. The most useful parameter for the determination of individual hot particle activity was found to be the intensity I, which corresponded to the approximate PSL_p value at the inflection point of the curve.

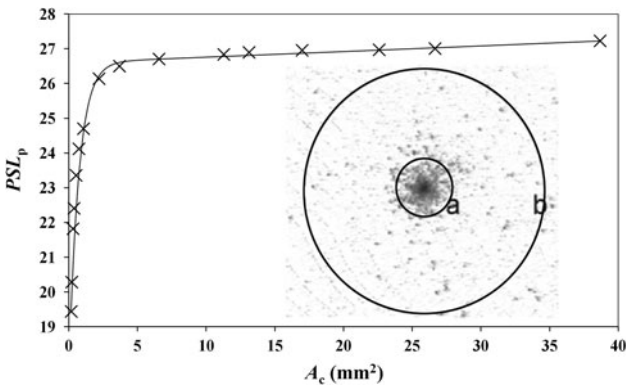

Fig. 3 Background-subtracted phosphor luminescence for particle T8poiA as a function of the size of the measurement area. The *inset* is an enlargement from a 1 h autoradiograph of T8poiA, field of view = 7 mm. "*a*" has an area $A_c = 1.26$ mm^2, and "*b*" $A_c = 22.82$ mm^2

$$PSL_p = I * e^{(b*A_c)} + c * e^{(f*A_c)} \quad (6)$$

where b is related to the slope of the function at the far right, found to be sensitive to the presence of nearby particles and background characteristics. c affects the A_c position of the inflection point. f is the sharpness of the inflection, related to the sample-to-plate geometry. Parameter f is related to the degree to which a hot particle is "focused".

In some cases, particles were so spatially crowded that a small A_c was required but was unsatisfactory when the activity was low, meaning the statistics were poor (just a few counts) within the area defined by A_c. In these cases it was desirable to use a slightly larger A_c offset from the center of the particle. The error introduced by the degree of offset was tested by comparing offset to PSL_p. Shifting the center of the area of measurement by 50–80 % of the radius varied the PSL_p value by 2–11 %, respectively. It is estimated that less than 5 % of the measurements used to produce the activity distribution were off-centered by more than 50 % of the radius of the measurement area.

Gamma spectrometry and imaging plate luminescence measurements corrected to the same measurement date found a linear relationship for the 17.5 ± 0.3 h case, which is described by Eq. 7. The standard deviation of the residuals of the data relative to the model was 0.0176 Bq.

$$\text{Activity in Bq} = 0.001 * I + 0.0102. r^2 = 0.95. \quad (7)$$

Using 17.5 ± 0.3 h autoradiographs of the dispersal tape preparation from section "e" of the inlet filter, 990 hot spots (hot particles) were measured, obtaining PSL_p for a given A_c from which I was solved using Eq. 6. The resulting I values were converted to Bq with Eq. 7 and plotted as a histogram, which is the activity distribution (Fig. 4). The distribution follows the Pareto power law distribution [12]. Most of the activity budget was represented by particles that fell below 50 mBq each. Examples of hot spots for individual hot particles are shown as insets in Fig. 4. Longer exposures of the same samples produced more hot spots since the lower detection limit was extended by the longer counting time. The greater abundance of particles detected by the longer counting times would have required additional dispersion to achieve accurate activity distributions extending to lower activity levels, but this seemed impractical to pursue without a reason to warrant the measurement of sub-mBq levels of particles.

A proportion of beta counts in the autoradiograph were not included in the distribution since they were either too dispersed to belong to a cluster, or formed hot spots that were too crowded to count accurately. When particles were too crowded to get reliable measurements, they were skipped. The combined errors of skipping particles, offset A_c selections and others were accounted for by two methods. The first error assessment was by comparing the final sum of the individually counted hot particles in PSL units against the total sum of phosphor luminescence in PSL units over the entire tape area (no skipping and no decentering). The second error assessment was by comparing the individual particle Bq measurements that were converted from the individual I measurements, to an independent gamma spectrometry measurement.

For the first error assessment, the sum of the distribution of I was 3,998 PSL. The complete tapes were 6,556 PSL. This suggests that 40 % of the measured activity was too dispersed or crowded to be counted. For the second error assessment, when summed the activity distribution for the August 18, 2011 measurement of filter piece "e" was 14 Bq. In comparison, gamma spectrometry on a filter piece 4 times the size of filter piece "e" was 46 Bq ($u_c = 4$ %). The uncertainty analysis of the 14 Bq sum of the 990 hot particles is a subject of further study by one of us, but at this time we can note that if this sum is multiplied by 4 so that the sizes of the filter pieces match, then the

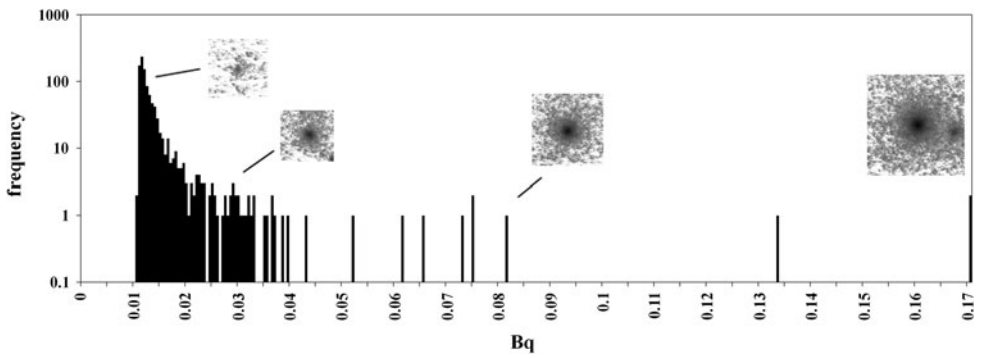

Fig. 4 Activity distribution in Bq as of August 18, 2011 when the autoradiography was performed, expressed as a log histogram for 990 particles measured in filter piece "e". The left hand shoulder on the peak (activities below 0.012 Bq) is partly attributed to difficulty in detecting the particles and does not necessarily relate to the true distribution. The *insets* are examples of the hot spots for four hot particles. Each is shown at the same scale, the rightmost being 20 mm wide. The hottest particle at the time of the measurement, 0.9 Bq plots off the scale

autoradiography measurements calibrated by gamma spectrometry (56 Bq) can be compared to the separate and single gamma spectrometry measurement on a separate single piece of filter (46 Bq). This level of difference is consistent with the stochastic nature of particle occurrence resulting in unequal loadings on the filter, but a more meaningful comparison awaits further uncertainty evaluations.

The $^{134}Cs/^{137}Cs$ ratio measured by gamma spectrometry on the hottest isolated particle (T8poiA, 0.9 Bq) corrected to March 20, 2011 was 0.90 ($u_c = 3$ %), whereas for another particle (0.03 Bq) it was 0.68 ($u_c = 28$ %). Other isolated particles had gamma-detectable ^{137}Cs at the 0.02 Bq level ($u_c = 20$ %), but the ^{134} Cs activity for these and lower activity particles fell below the gamma spectrometry detection limit and ratios could not be obtained. Groupings of particles to achieve levels above the gamma detection limits produced date-corrected activity ratios of 0.82 ($u_c = 12$ %), 0.97 ($u_c = 5$ %), 1.01 ($u_c = 5$ %), 1.09 ($u_c = 11$ %) and 1.29 ($u_c = 15$ %). A representative eighth of the original inlet filter equivalent to the average of several thousand particles had a date-corrected ratio of 0.92 ($u_c = 4$ %).

Conclusions

A new method is presented for obtaining activity distributions by nondestructive dry preparation and analysis based on autoradiography and conventional nuclear counting. Autoradiography-based measures were developed that are indicative of sample-to-plate geometry, spatial crowding and activity. Aerosols collected in Japan shortly after the 2011 tsunami were rich in $^{137+134}Cs$-bearing particles. Approximately 1,000 particles detected in a 17.5 h autoradiograph of a 2.7 cm^2 filter area (roughly 10^4 m^3 air) ranged from a few mBq to close to 1 Bq each. The most active particle corresponded to a minimum equivalent diameter of about 0.5 μm. The lower their activity, the more abundant the particles were. The greatest activity component fell below 50 mBq per particle in the sample analyzed. The lower range of the measurable distribution was a function of autoradiography exposure time, but an overnight autoradiograph appeared to achieve a reasonable lower distribution limit. Alpha activity above background was not detected. The average $^{134}Cs/^{137}Cs$ activity ratio date-corrected to March 20, 2011 was 0.92 ($u_c = 4$ %). Results support other efforts to analyze emissions from Fukushima and environmental contaminants [13–18] and other autoradiography measurements [19, 20].

References

1. Nuclear Energy Agency (2001) http://www.oecd-nea.org/press/2011/NEWS-04.html. Accessed 24 Aug 2011
2. Nikkinen M et al (2011) CTBTO science and technology 201,#JS-09, Vienna, Austria, 8–10 June 2011
3. Williams M (2011) IDG News Service http://www.arnnet.com.au/article/384238/ us_roboticists_complete_mission_japan_tsunami-hit_coast. Accessed 10 Feb 2012
4. Lindstrom RM (1994) Biol Trace Elem Res 43–45:597–603
5. Pollanen R et al (2011) J Radioanal Nucl Chem 248:623–627
6. Fichet P et al (2012) J Radioanal Nucl Chem 291:869–875
7. Zeissler CJ (2009) Log 315. MARC VIII, Kona
8. Zeissler CJ, Lindstrom AP, Davis J (2011) NUCL-33. American Chemical Society, Denver
9. Zeissler CJ, Lindstrom AP (2010) Nucl Instrum Meth Phys Res A 624:92–100
10. Amemiya Y, Miyahara J (1988) Nature 336:89–90
11. Ohuchi H, Yamadera A (2002) Nucl Instrum Meth Phys Res A 490:573–582
12. Vidonodo B et al (1997) Limnol Oceanogr 42:184–192
13. Changlai SP et al (2012) J Radioanal Nucl Chem 291:859–863
14. Tagami K et al (2012) J Radioanal Nucl Chem 292:243–247
15. Manolopoulou M et al (2012) J Radioan Nucl Chem 292:155–159
16. Jinglong Wang et al (2012) J Radioanal Nucl Chem 292:1297–1301
17. Sartandel S et al (2012) J Radioanal Nucl Chem 292:995–998
18. Akio Iwanade et al (2012) J Radioanal Nucl Chem 293:703–709
19. Stanley FE et al (2012) J Radioanal Nucl Chem. doi: 10.1007/s10967-012-1927-3
20. Fichet P et al (2012) J Radioanal Nucl Chem 291:869–875